



## Novel computational methods based on Bernoulli operational matrix for time-space fractional advection-dispersion equation

Hamid Reza Khodabandehlo<sup>a</sup>, Elyas Shivanian<sup>a,\*</sup>, Tannaz Godarzvand Chegini<sup>b</sup>

<sup>a</sup>Department of Applied Mathematics, Faculty of Science, Imam Khomeini International University, Qazvin, 34149, Iran.

<sup>b</sup>Department of Mathematical Sciences, Montana State University, Bozeman, MT 59717, USA.

### Abstract

This article investigates the time-space fractional advection-dispersion equation (TSAFE). In this work, an efficient and precise numerical method (Novel Bernoulli Operational Matrix technique) is applied for solving a category of these equations, converting the original problem into a set of algebraic equations that can be solved using numerical methods. The key benefit of this scheme is its ability to transform linear and nonlinear (PDEs) into a set of algebraic equations concerning the expansion coefficients of the solution. The suggested scheme is effectively utilized for the mentioned problem. Sufficient and thorough numerical evaluations are provided to illustrate the precision, applicability, effectiveness, and adaptability of the introduced scheme. To showcase the efficacy and accuracy of this technique, the numerical results from the examples are expressed in a table format to enable comparison with results from other established methods as well as with the precise solutions. It should be noted that the implementation of the current method is regarded as quite simple.

**Keywords:** Operational matrix, Time-space fractional diffusion equation, Caputo differential operator, Bernoulli polynomials.

**2020 MSC:** 65L99, 34A08.

©2026 All rights reserved.

### 1. Introduction

The uses and study of fractional order calculus have been vibrant and among the quickest expanding fields of research over the past thirty years. It has now turned into a vital instrument owing to its extensive application across various scientific fields, including blood flow dynamics, biophysics, chemistry, physics, ongoing thermodynamic variations, the electro-dynamics of complex materials, capacitor principles, polymer rheology, dynamic systems, experimental data fitting, and more ([11, 14, 32, 5, 17, 38, 37, 54, 26, 36, 39] and references therein). The growing advancement of suitable and effective techniques for addressing fractional differential equations (FDEs) has generated heightened interest among scholars in this area. Owing to the various uses of these equations, several techniques have been developed to solve them, including Fractional Adams-Moulton methods [21], fractional linear multi-steps methods [43], trapezoidal methods [23], and many others.

\*Corresponding author

Email address: [shivanian@sci.ikiu.ac.ir](mailto:shivanian@sci.ikiu.ac.ir) (Elyas Shivanian<sup>✉</sup>)

doi: [10.30511/mcs.2026.2067111.1421](https://doi.org/10.30511/mcs.2026.2067111.1421)

Received: 26 July 2025 Accepted: 21 April 2026

Numerous researchers investigated the fractional advection-dispersion equation (ADE) recently. Our objective is to examine the time-space fractional ADE. Space nonlocality relates to long-range interactions, while time nonlocality pertains to memory effects. The Time-Space Advection-Dispersion Equation (TSFADE) outlines the movement of materials, such as contaminants in groundwater, by taking into account both advection (large-scale flow) and dispersion (distribution). It's a broadening of the traditional ADE, frequently integrating fractional derivatives to address unusual diffusion and advection. The ADE and its fractional variants are commonly employed to represent solute movement in porous media, such as groundwater aquifers. They are essential for grasping and forecasting. Fractional models are particularly useful when the transport mechanism exhibits anomalous diffusion, which contrasts with conventional Fickian diffusion. The core concept is that fractional order models provide greater insight into the underlying structure and behavior of complex systems. Essentially, the time-space fractional ADE offers a more adaptable and precise framework for representing transport processes by utilizing fractional calculus to explain anomalous diffusion and advection effects. Because of the intricacy of fractional derivatives, numerical techniques are frequently required to address the fractional ADEs. A range of techniques has been created to solve these equations, such as spectral methods, finite element methods, finite difference methods, and more [29, 64, 47, 56, 2, 42, 41, 20, 24, 12]. Recently, various numerical schemes have been created for the FADE, the majority of them concerning time FADEs [3, 22, 49, 53, 58, 30, 61, 65], while several focus on space FADEs [55, 48, 57, 62, 35, 25]. Nevertheless, there exist certain physical issues that are represented with both spatial and temporal FADEs such as TSF Fokker-Planck equation, serving as a powerful instrument for processes involving both flights and traps, where the space fractional term describes the flights and the time fractional component defines the traps [29, 64, 47, 56, 2, 12, 28, 45, 16, 27, 41, 10]. Despite this and because of the fact that the numerical techniques for these issues are quite difficult, and numerous numerical techniques have been created for these equations.

Finding exact solutions for the majority of FDEs is not straightforward, leading to the need for analytical and numerical techniques to be employed. On the other hand, it is known that acquiring analytical solutions to these equations is quite challenging. Therefore, in many cases, the precise solution remains unknown, and it is necessary to pursue a numerical estimation. Consequently, numerous investigators have devised and advanced numerical techniques to facilitate to acquire estimated solutions for this category of equations.

Recently, Bernoulli polynomials have demonstrated their strength as a mathematical tool for addressing involving a range of dynamic issues, such as numerically addressing high-order Fredholm integro-differential equations [9], pantograph equations [59], PDEs [60], linear Volterra and nonlinear Volterra-Fredholm-Hammerstein IEs [6], alongside optimal control challenges [31], variable-order FDEs [46, 33] and nonlinear multi-term fractional variable-order delay differential equation [34].

As far as we know, there has not been any numerical method created utilizing the Bernoulli Operational Matrix approach for the TSFADEs. At present, the primary objective of this article is to generalize the classical polynomials in the foundation of the solution. We propose a Novel Operational Matrix technique that relies on Bernoulli polynomials to compute the solution of TSFADEs numerically. This approach employs the (NBOM) method to convert the main problem into a system of algebraic equations that can be solved by well-known numerical methods. Thus, we present a (NBOM) for the derivatives of fractional order for solving a category of TSFADEs which as follow:

$$\frac{\partial^\gamma z(x, t)}{\partial t^\gamma} = \kappa_1 \frac{\partial^n z(x, t)}{\partial x^n} - \kappa_2 \frac{\partial^\zeta z(x, t)}{\partial x^\zeta} + h(x, t), \quad 0 < x < X_R, \quad 0 < t < \infty, \quad (1.1)$$

with boundary and initial conditions

$$z(0, t) = a_1(t), \quad z(X_R, t) = a_2(t), \quad t > 0, \quad (1.2)$$

$$z(x, 0) = b(x), \quad 0 < x < X_R. \quad (1.3)$$

where the spatial coordinates  $x$  and  $t$  signifies time,  $z(x, t)$  is the unknown function that must be estimated as the solute concentration,  $0 < \gamma < 1$  represents the temporal order,  $1 < \eta < 2, 1 < \zeta < 1$  are the orders of spatial fractional derivatives and  $\kappa_1, \kappa_2$  are the positive constants that represent the anomalous dispersion and advection coefficients, respectively. The function  $h(x, t)$  represents a given function (as the source term), the initial value is  $b(x)$  and  $a_1(t)$  and  $a_2(t)$  are prescribed boundary functions (as the boundary solute concentrations). Additionally, the operators  $\frac{\partial^\gamma z(x, t)}{\partial t^\gamma} = D_t^\gamma, \frac{\partial^i z(x, t)}{\partial x^i} = D_x^i, i = \eta, \zeta$  are the Caputo's fractional order derivatives for time and space. It is evident that if  $\gamma = 1, \eta = 2, \zeta = 1$ , then equations (1.1)-(1.3) will be classical ADE.

## 2. Preliminaries

This section first reviews foundational concepts in fractional calculus. We then examine significant properties of Bernoulli polynomials, which form the basis for the proposed method.

### 2.1. The fractional order derivative

Various definitions exist and are utilized for the fractional derivative, yet the three most common definitions of them are presented by Caputo, Grünwald-Letincov, and Riemann-Liouville. Due to the Caputo fractional derivative is the only model that behaves like the integer-order DE, in this article we use it.

**Definition 2.1.** The  $\zeta$ -order ( $m - 1 < \zeta \leq m$ ) fractional derivatives of Caputo (right and left-sided) are presented as

$$D_-^\zeta z(x) = \frac{(-1)^m}{\Gamma(m - \zeta)} \int_x^{x_R} \frac{z'(s)}{(s - x)^{\zeta - m + 1}} ds, \tag{2.1}$$

$$D_+^\zeta z(x) = \frac{1}{\Gamma(m - \zeta)} \int_0^x \frac{z'(s)}{(x - s)^{\zeta - m + 1}} ds,$$

that

$$D_+^\zeta x^w = \begin{cases} 0, & \text{for } w \in M_0 \text{ and } w < \lceil \zeta \rceil, \\ \frac{\Gamma(w + 1)}{\Gamma(w - \zeta + 1)} x^{w - \zeta}, & \text{for } w \in M_0 \text{ and } w > \lceil \zeta \rceil, \end{cases} \tag{2.2}$$

and

$$D_-^\zeta (X_R - x)^w = \begin{cases} 0, & \text{for } w \in M_0 \text{ and } w < \lceil \zeta \rceil, \\ \frac{(-1)^w \Gamma(w + 1)}{\Gamma(w - \zeta + 1)} (X_R - x)^{w - \zeta}, & \text{for } w \in M_0 \text{ and } w > \lceil \zeta \rceil, \end{cases} \tag{2.3}$$

where  $M_0 = \{0, 1, 2, \dots\}$  and  $\lceil \cdot \rceil$  is the ceiling function. Also

$$D_\pm^\zeta (\gamma\phi(x) + \delta\phi(x)) = \gamma D_\pm^\zeta (\phi(x)) + \delta D_\pm^\zeta (\phi(x)),$$

where  $\gamma$  and  $\delta$  are constants.

### 2.2. Bernoulli Polynomials and their properties

The polynomials of Bernoulli form a set of independent polynomials that constitute a complete basis for all square-integrable function spaces over the interval  $[0, 1]$  (known as the space  $L^2[0, 1]$ ).

Let  $B_n(s)$  represents the  $n$ -th degree Bernoulli polynomial in  $s$ , is described as follows [46, 13]:

$$B_n(s) = \sum_{j=0}^n \binom{n}{j} b_{n-j} s^j, \tag{2.4}$$

where  $b_j, j = 0, 1, \dots, n$ , denote the numbers of Bernoulli that found in the series expansion of trigonometric functions [46, 1] and can be characterized using the subsequent identification:

$$\frac{s}{e^s - 1} = \sum_{j=0}^{\infty} b_j \frac{s^j}{j!}, \quad (2.5)$$

thus

$$\begin{aligned} B_0(s) &= 1, \\ B_1(s) &= s - \frac{1}{2}, \\ B_2(s) &= s^2 - s + \frac{1}{6}, \\ B_3(s) &= s^3 - \frac{3}{2}s^2 + \frac{1}{2}s, \\ B_4(s) &= s^4 - 2s^3 + s^2 - \frac{1}{30}, \end{aligned}$$

the initial five Bernoulli polynomials.

The subsequent property holds for Bernoulli polynomials [1]:

$$\int_0^1 B_k(s) B_m(s) = (-1)^{-1+k} \frac{m! k!}{(m+k)!} b_{m+k}, \quad m, k \geq 1.$$

Conversely, the Bernoulli polynomials can be conveniently produced using the subsequent recursive relation

$$\sum_{j=0}^{n-1} \binom{n}{j} B_j(s) = ns^{n-1}, \quad j = 2, 3, \dots. \quad (2.6)$$

We remember that the benefits of Bernoulli polynomials in estimating any unknown arbitrary function, compared to certain traditional orthogonal polynomials, are:

- I. The operational matrix of derivatives for Bernoulli contains fewer nonzero elements compared to that of some shifted classical orthogonal polynomials. The nonzero entries of the Bernoulli operational matrix exist solely in the first subdiagonal. In contrast, the shifted Jacobi and Chebyshev polynomials form a strictly lower triangular matrix, as noted in [19, 18].
- II. The Bernoulli polynomials contain fewer terms than the some classical orthogonal polynomials. For instance, the sixth Bernoulli polynomial contains five terms, whereas the sixth shifted Chebyshev polynomial consists of seven terms, and this disparity will grow as the degree increases. Thus, when approximating any arbitrary function, we utilize more CPU time by employing classical orthogonal polynomials in contrast to Bernoulli polynomials; for further reading refer to [44].
- III. The coefficients of separate terms in Bernoulli polynomials are less than such coefficients in the classical orthogonal polynomials. As the calculation errors in the product are tied to the coefficients of separate terms, employing Bernoulli polynomials reduces these errors.

Therefore, considering the above-mentioned issues and due to its high accuracy and easy implementation, using Bernoulli operational matrix method is economical.

### 3. Approximating function using Bernoulli polynomials

Assume the function  $z(x)$  is square integrable relative to  $\omega_{X_R}^{(\alpha,\beta)}(x)$  on the interval  $[0, X_R]$ , consequently, it can be stated in the following manner[46]:

$$z(x) = \sum_{j=0}^{\infty} f_j B_{X_R,j}(x), \tag{3.1}$$

where  $f_j$  (the coefficients of the series ) are obtained using the formula presented in [6, 31] as follows:

$$f_j = \frac{1}{j!} \int_0^1 \frac{d^j z(x)}{dx^j} dx. \tag{3.2}$$

Thus, we can approximate the solution utilizing  $(M + 1)$ -terms of the given series in Eq. (3.1) and we shall possess

$$z(x) \simeq z_M(x) = \sum_{j=0}^M f_j B_{X_R,j}(x) = F^T \Phi_{X_R,M}(x), \tag{3.3}$$

where  $F = [f_0, f_1, \dots, f_M]^T$ , and  $\Phi_{X_R,M}(x) = [B_{X_R,0}(x), B_{X_R,1}(x), \dots, B_{X_R,M}(x)]^T$ .

Here, we assume that

$$S(x) = [1, x, x^2, x^3, \dots, x^M]^T.$$

By Eq.(3.3), the vector  $\Phi_{X_R,M}(x)$  can be shown as

$$\Phi_{X_R,M}(x) = \begin{bmatrix} B_{X_R,0}(x) \\ B_{X_R,1}(x) \\ \vdots \\ B_{X_R,i}(x) \\ \vdots \\ B_{X_R,M}(x) \end{bmatrix} = \begin{bmatrix} b_0 \\ \sum_{k=0}^1 \binom{1}{k} b_{1-k} x^k \\ \vdots \\ \sum_{k=0}^i \binom{i}{k} b_{i-k} x^k \\ \vdots \\ \sum_{k=0}^M \binom{M}{k} b_{M-k} x^k \end{bmatrix} \tag{3.4}$$

$$= \begin{bmatrix} \theta_{1,1} & \theta_{1,2} & \cdots & \theta_{1,M+1} \\ \theta_{2,1} & \theta_{2,2} & \cdots & \theta_{2,M+1} \\ \vdots & \vdots & \vdots & \vdots \\ \theta_{i,1} & \theta_{i,2} & \cdots & \theta_{i,M+1} \\ \vdots & \vdots & \vdots & \vdots \\ \theta_{M+1,1} & \theta_{M+1,2} & \cdots & \theta_{M+1,M+1} \end{bmatrix} \begin{bmatrix} 1 \\ x \\ \vdots \\ x^i \\ \vdots \\ x^M \end{bmatrix} = \Theta S(x),$$

where  $\Theta$  is a square matrix (of dimensions  $(M + 1) \times (M + 1)$  ) described as follows

$$\theta_{l+1,k+1} = \begin{cases} \binom{l}{k} b_{l-k}, & l \geq k, \\ 0, & \text{otherwise,} \end{cases} \tag{3.5}$$

for  $0 \leq l, k \leq M$ .

Then  $\Theta$  as follows

$$\Theta = \begin{bmatrix} 1 & 0 & 0 & 0 & 0 & \cdots & 0 \\ -\frac{1}{2} & 1 & 0 & 0 & 0 & \cdots & 0 \\ \frac{1}{6} & -1 & 1 & 0 & 0 & \cdots & 0 \\ 0 & \frac{1}{2} & -\frac{3}{2} & 1 & 0 & \cdots & 0 \\ \vdots & \vdots & \vdots & \vdots & \vdots & \cdots & 0 \\ b_M & \binom{M}{1} b_{M-1} & \binom{M}{2} b_{M-2} & \binom{M}{3} b_{M-3} & \binom{M}{4} b_{M-4} & \cdots & 1 \end{bmatrix}. \quad (3.6)$$

Hence, using Eq. (3.4), we get

$$S(x) = \Theta^{-1} \Phi_{X_R, M}(x). \quad (3.7)$$

In the same way, a function  $z(x, t)$  that depends on two independent variables defined for  $0 < t \leq T < \infty$  and  $0 < x < X_R$  can be expressed using the double Bernoulli polynomials as:

$$z(x, t) \simeq z_{N, M}(x, t) = \sum_{i=0}^M \sum_{j=0}^N a_{ij} B_{T, i}(t) B_{X_R, j}(x) = \Phi_{T, M}^T(t) A \Phi_{X_R, N}(x), \quad (3.8)$$

where

$$\begin{aligned} \Phi_{T, M}(t) &= [B_{T, 0}(t), B_{T, 1}(t), \dots, B_{T, M}(t)]^T, \\ \Phi_{X_R, N}(x) &= [B_{X_R, 0}(x), B_{X_R, 1}(x), \dots, B_{X_R, N}(x)]^T \end{aligned}$$

and

$$A = \begin{bmatrix} a_{00} & a_{01} & a_{02} & \cdots & a_{0N} \\ a_{10} & a_{11} & a_{12} & \cdots & a_{1N} \\ \vdots & \vdots & \vdots & \cdots & \vdots \\ a_{M0} & a_{M1} & a_{M2} & \cdots & a_{MN} \end{bmatrix}. \quad (3.9)$$

where the coefficients  $a_{lr}, l = 0, 1, \dots, M, r = 0, 1, \dots, N$ . must be estimated.

#### 4. Novel Bernoulli Polynomials Operational Matrix (NBOM)

Operational matrices, utilized across various fields of numerical analysis, address diverse issues of various kinds and subjects are particularly significant, including IEs, DEs, and integro-differential equations, partial and ordinary FDEs [10, 63, 40, 50, 15, 7, 52, 51, 4, 8]. Now, we explore the (NBOM) of fractional order to assist in the computational solution of Eq.(1.1). Thus, we transform the original problem into a set of algebraic equations that can be solved using numerical techniques in collocation points.

Initially, we infer

$$D_x^\zeta \Phi_{X_R, N}(x) \quad (m - 1 < \zeta \leq m, m \in \mathbb{N})$$

as follows:

based on the previous content, have:  $\Phi_{X_R, N}(x) = \Theta_x S(x)$ , so

$$D_x^\zeta \Phi_{X_R, N}(x) = D_x^\zeta (\Theta_x S(x)) = \Theta_x D_x^\zeta [1, x, \dots, x^N]^T. \quad (4.1)$$

Combining Eqs. (2.2) and (4.1), in general, it gives:

$$\begin{aligned}
 D_x^\zeta \Phi_{X_R, N}(x) &= \Theta_x D_x^\zeta (S(x)) \\
 &= \Theta_x [0, \dots, 0, \frac{\Gamma([\zeta] + 1)x^{([\zeta] - \zeta)}}{\Gamma([\zeta] + 1 - \zeta)}, \dots, \frac{\Gamma(N + 1)x^{(N - \zeta)}}{\Gamma(N + 1 - \zeta)}]^T \\
 &= \Theta_x \begin{bmatrix} 0 & \dots & 0 & 0 & 0 & \dots & 0 \\ \vdots & \dots & \vdots & \vdots & \vdots & \dots & \vdots \\ 0 & \dots & 0 & 0 & 0 & \dots & 0 \\ 0 & \dots & 0 & \frac{\Gamma([\zeta] + 1)x^{-\zeta}}{\Gamma([\zeta] + 1 - \zeta)} & 0 & \dots & 0 \\ 0 & \dots & 0 & 0 & \frac{\Gamma([\zeta] + 2)x^{-\zeta}}{\Gamma([\zeta] + 2 - \zeta)} & \dots & 0 \\ \vdots & \dots & \vdots & \vdots & \vdots & \ddots & \vdots \\ 0 & \dots & 0 & \dots & \dots & 0 & \frac{\Gamma(N + 1)x^{-\zeta}}{\Gamma(N + 1 - \zeta)} \end{bmatrix} \begin{bmatrix} 1 \\ x \\ \vdots \\ x^{[\zeta]} \\ x^{[\zeta] + 1} \\ \vdots \\ x^N \end{bmatrix} \\
 &= \Theta_x G_{\zeta_x} S(x).
 \end{aligned}$$

Where

$$G_{\zeta_x} = \begin{bmatrix} 0 & \dots & 0 & 0 & 0 & \dots & 0 \\ \vdots & \dots & \vdots & \vdots & \vdots & \dots & \vdots \\ 0 & \dots & 0 & 0 & 0 & \dots & 0 \\ 0 & \dots & 0 & \frac{\Gamma([\zeta] + 1)x^{(-\zeta)}}{\Gamma([\zeta] + 1 - \zeta)} & 0 & \dots & 0 \\ 0 & \dots & 0 & 0 & \frac{\Gamma([\zeta] + 2)x^{(-\zeta)}}{\Gamma([\zeta] + 2 - \zeta)} & \dots & 0 \\ \vdots & \dots & \vdots & \vdots & \vdots & \ddots & \vdots \\ 0 & \dots & 0 & \dots & \dots & 0 & \frac{\Gamma(N + 1)x^{-\zeta}}{\Gamma(N + 1 - \zeta)} \end{bmatrix}.$$

in other words

$$[G_{\zeta_x}]_{i,j} = \begin{cases} \frac{\Gamma(i)}{\Gamma(i - \zeta)} x^{(-\zeta)}, & \text{for } [\zeta] + 1 \leq i \leq N, \quad i = j, \\ 0, & \text{otherwise.} \end{cases} \tag{4.2}$$

Using Eq. (3.7), then

$$D_x^\zeta \Phi_{X_R, N}(x) = \Theta_x G_{\zeta_x} \Theta_x^{-1} \Phi_{X_R, N}(x).$$

The operational matrix of  $D_x^\zeta \Phi_{X_R, N}(x)$  is  $\Theta_x G_{\zeta_x} \Theta_x^{-1}$ .

Not that accordingly, if  $\zeta = n$  ( $n$  is an integer) then we will have

$$[G_{\zeta_x}]_{i,j} = \begin{cases} \frac{\Gamma(i)}{\Gamma(i - n)} x^{-n}, & \text{for } n + 1 \leq i \leq N, \quad i = j, \\ 0, & \text{otherwise.} \end{cases} \tag{4.3}$$

Note that in  $D_x^\zeta$ , the first  $[\zeta] = m$  rows are all zero.

Here, we approximate the fractional order derivative of the function derived in Eq. (3.3) in the following way:

$$\begin{aligned} D_x^\zeta z(x) &\simeq D_x^\zeta (F^T \Phi_{X_R,N}(x)) = F^T D_x^\zeta \Phi_{X_R,N}(x) \\ &= F^T \Theta_x G_{\zeta_x} \Theta_x^{-1} \Phi_{X_R,N}(x). \end{aligned} \tag{4.4}$$

Now, we estimate  $z(x, t)$ ,  $h(x, t)$  by the shifted Jacobi polynomials as

$$\begin{aligned} z(x, t) &\simeq z_{N,M}(x, t) = \sum_{i=0}^M \sum_{j=0}^N \alpha_{ij} B_{T,i}(t) B_{X_R,j}(x) = \Phi_{T,M}^T(t) A \Phi_{X_R,N}(x), \\ h(x, t) &\simeq h_{N,M}(x, t) = \sum_{i=0}^M \sum_{j=0}^N h_{ij} B_{T,i}(t) B_{X_R,j}(x) = \Phi_{T,M}^T(t) H \Phi_{X_R,N}(x). \end{aligned} \tag{4.5}$$

where matrix  $A$  is an unknown  $((M + 1) \times (N + 1))$  which is shown in Eq. (3.9), but the matrix  $H$  is known and is as follows:

$$H = \begin{bmatrix} h_{00} & h_{01} & \cdots & h_{0N} \\ h_{10} & h_{11} & \cdots & h_{1N} \\ \vdots & \vdots & \cdots & \vdots \\ h_{M0} & h_{M1} & \cdots & h_{MN} \end{bmatrix}$$

which coefficients  $h_{ij}, i = 0, 1, \dots, M, j = 0, 1, \dots, N$  can be calculated using the formula presented in [6, 31].

By using Eqs. (4.2) and (4.4), hence the equation (1.1) turned into

$$\begin{aligned} D_t^\gamma (\Phi_{T,M}^T(t) A \Phi_{X_R,N}(x)) &= \kappa_1 D_x^\eta (\Phi_{T,M}^T(t) A \Phi_{X_R,N}(x)) - \kappa_2 D_x^\zeta (\Phi_{T,M}^T(t) A \Phi_{X_R,N}(x)) + (\Phi_{T,M}^T(t) H \Phi_{X_R,N}(x)), \\ \implies (D_t^\gamma \Phi_{T,M}^T(t) A \Phi_{X_R,N}(x)) &= \kappa_1 \Phi_{T,M}^T(t) A (D_x^\eta \Phi_{X_R,N}(x)) - \kappa_2 \Phi_{T,M}^T(t) A (D_x^\zeta \Phi_{X_R,N}(x)) + (\Phi_{T,M}^T(t) H \Phi_{X_R,N}(x)), \end{aligned}$$

then

$$\begin{aligned} (\Phi_{T,M}^T(t) \Theta_t^{-1} G_{\gamma_t} \Theta_t) A \Phi_{X_R,N}(x) &= \kappa_1 \Phi_{T,M}^T(t) A (\Theta_x G_{\eta_x} \Theta_x^{-1} \Phi_{X_R,N}(x)) \\ &- \kappa_2 \Phi_{T,M}^T(t) A (\Theta_x G_{\zeta_x} \Theta_x^{-1} \Phi_{X_R,N}(x)) + (\Phi_{T,M}^T(t) H \Phi_{X_R,N}(x)). \end{aligned} \tag{4.6}$$

with boundary and initial conditions

$$\begin{aligned} \Phi_{T,M}^T(t) A \Phi_{X_R,N}(0) &= a_1(t), \quad 0 < t < T, \\ \Phi_{T,M}^T(t) A \Phi_{X_R,N}(X_R) &= a_2(t), \quad 0 < t < T, \\ \Phi_{T,M}^T(0) A \Phi_{X_R,N}(x) &= b(x), \quad 0 < x < X_R. \end{aligned}$$

Ultimately, we utilize  $t_l = \frac{T(2l + 1)}{(2M + 2)} (l = 0, 1, 2, \dots, M)$  and  $x_j = \frac{T(2j + 1)}{(2N + 2)} (j = 0, 1, \dots, N)$  where they are the collocation points. Consequently Eq. (4.6) converted into the following form

$$\begin{aligned} (\Phi_{T,M}^T(t_l) \Theta_t^{-1} G_{\gamma_t} \Theta_t) A \Phi_{X_R,N}(x_j) &= \kappa_1 \Phi_{T,M}^T(t_l) A (\Theta_x G_{\eta_x} \Theta_x^{-1} \Phi_{X_R,N}(x_j)) \\ &- \kappa_2 \Phi_{T,M}^T(t_l) A (\Theta_x G_{\zeta_x} \Theta_x^{-1} \Phi_{X_R,N}(x_j)) + (\Phi_{T,M}^T(t_l) H \Phi_{X_R,N}(x_j)), \\ l = 1, 2, \dots, M, \quad j = 1, 2, \dots, N - 1. \end{aligned} \tag{4.7}$$

and we get  $M \times (N - 1)$  linear algebraic equations.

On the other hand, by the boundary and initial conditions,  $(2M + N + 1)$  linear algebraic equations by collocating these three equations at the zeros  $t_l$  and  $x_j$  are generated.

$$\begin{aligned} \Phi_{T,M}^T(0) A \Phi_{X_R,N}(x_j) &= b(x_j), \quad j = 1, 2, \dots, N - 1, \\ \Phi_{T,M}^T(t_l) A \Phi_{X_R,N}(0) &= a_1(t_l), \quad l = 0, 1, 2, \dots, M, \\ \Phi_{T,M}^T(t_l) A \Phi_{X_R,N}(X_R) &= a_2(t_l), \quad l = 0, 1, 2, \dots, M. \end{aligned} \tag{4.8}$$

Therefore, in total, we have  $(M + 1) \times (N + 1)$  equations and  $(M + 1) \times (N + 1)$  unknowns, so, we can solve the linear algebraic system in Eqs. (4.7) and (4.8) numerically for determining the matrix  $A$ . Therefore, the numerical solution that presented in Eq. (3.8) can be obtained.

## 5. Numerical results

By solving some examples in this section, we show the efficiency of the method by using the Mathematica 13 software.

These examples have been examined in terms of maximum Absolute Error ( $E_A = \max_{0 \leq i \leq N} |z_{\text{Exact}}(x_i, t) - z_{N,M}(x_i, t)|$ ) and the CPU time required for solving them.

Comparison of the outcomes produced by this method with the precise solution and with various other methods (available in the literature) for each example indicates that this innovative technique align most closely with the exact solution. The stability, consistency and straightforward application of this technique make this method to be more usable and dependable.

**Example 5.1.** Consider the following TSFADE[29]:

$$\begin{aligned} \frac{\partial^\gamma z(x, t)}{\partial t^\gamma} &= \kappa_1 \frac{\partial^\eta z(x, t)}{\partial x^\eta} - \kappa_2 \frac{\partial^\zeta z(x, t)}{\partial x^\zeta} + h(x, t), \quad 0 < t < 1, \quad 0 < x < 1, \\ z(x, 0) &= x^2(1-x)^2, \quad 0 < x < 1, \\ z(0, t) &= z(1, t) = 0, \quad 0 < t < 1, \end{aligned} \quad (5.1)$$

Note that  $z(x, t) = x^2(1-x)^2 e^{-t}$  is the exact solution,  $\kappa_1 = 0.001$ ,  $\kappa_2 = 2$ .

Utilizing the ideas outlined in Section 4, we regard the approximate solution featuring  $(M+1) \times (N+1)$  finite terms shown in Eq. (3.8) for this problem and replace in primary problem. Then by applying the Eq. (4.4), this problem is transformed into form of the Eq. (4.6), finally using  $t_i$  and  $x_j$ , therefore, an equations system emerges that we can solve it by known numerical techniques to obtain the unknown matrix A.

The maximum Absolute Errors (at some nodal points) of this method, as well as the CPU time needed for it, are given in Table (1). From this Table, it is observed that the numerical results are very close to the exact solution and Figure (1) confirms the reliability of NBOM method compared to other techniques. Moreover, in Figure (2) we plot the Absolute error for this example. Note that the Figures (1) and (2) show a proper match between the approximate solutions and the exact solution.

Therefore, it follows that the solution of the Eq. (5.1), approximated using new method, is in the best agreement with the accurate solution.

In addition, Tables (2) and (3) show  $E_2^T = \|z_{\text{Exact}}(x, T) - z_{N,M}(x, T)\|_2$  and  $E_\infty^T = \|z_{\text{Exact}}(x, T) - z_{N,M}(x, T)\|_\infty$  errors at  $T = 1$  for different values of  $1 \leq \eta \leq 2$ .

Also experimental rate of convergence  $\frac{\log(\frac{E_s}{E_{s+1}})}{\log(\frac{N_{s+1}}{N_s})}$  (where  $E_{s+1}$  and  $E_s$  are the errors corresponding to

$N_{s+1}$  and  $N_s$ ) is provided in these tables and compare the accuracy and efficiency of our method and method in [29]. It is seen that the our technique is better than method in [29].

**Example 5.2.** Consider the following TSFADE[28]:

$$\begin{aligned} \frac{\partial^\gamma z(x, t)}{\partial t^\gamma} &= \kappa_1 \frac{\partial^\eta z(x, t)}{\partial x^\eta} - \kappa_2 \frac{\partial^\zeta z(x, t)}{\partial x^\zeta} + h(x, t), \quad 0 < t < 1, \quad 0 < x < 1, \\ z(x, 0) &= x^2, \quad 0 < x < 1, \\ z(0, t) &= t^2, \quad \frac{\partial z}{\partial x}(0, t) = 0, \quad 0 < t < 1, \end{aligned} \quad (5.2)$$

Note that  $z(x, t) = x^2 + t^2$  is the exact solution,  $\kappa_1 = \kappa_2 = 1$ .

Like the previous example, in this example, the maximum absolute errors (at some nodal points) of this method, also the CPU time needed for our method are given and compared in Table (4), confirming

Table 1: Comparison the absolute errors at some nodal points for Ex.1 with  $\gamma = 1, \zeta = 0.5$  and different values of  $\eta$  at  $T = 1$ .

$x \in [0, X_R]$	$\eta$	Current technique ( $Z_{4,8}$ )	$\eta$	Current technique ( $Z_{4,8}$ )
0	1.2	$3.80 \times 10^{-13}$	1.6	$1.86 \times 10^{-12}$
0.1	1.2	$6.47 \times 10^{10}$	1.6	$2.65 \times 10^{-11}$
0.2	1.2	$2.56 \times 10^{-10}$	1.6	$4.70 \times 10^{-11}$
0.3	1.2	$2.27 \times 10^{-10}$	1.6	$1.22 \times 10^{-10}$
0.4	1.2	$4.60 \times 10^{-9}$	1.6	$5.60 \times 10^{-10}$
0.5	1.2	$1.07 \times 10^{-8}$	1.6	$1.41 \times 10^{-9}$
0.6	1.2	$1.30 \times 10^{-8}$	1.6	$2.27 \times 10^{-9}$
0.7	1.2	$7.85 \times 10^{-9}$	1.6	$2.44 \times 10^{-9}$
0.8	1.2	$1.18 \times 10^{-9}$	1.6	$1.53 \times 10^{-9}$
0.9	1.2	$3.95 \times 10^{-9}$	1.6	$1.08 \times 10^{-10}$
1.0	1.2	$4.19 \times 10^{-13}$	1.6	$1.84 \times 10^{-12}$
CPU time	-	1.56 s	-	1.46 s

Table 2: Error norms and experimental order of convergence for different values of  $\eta$  at  $T = 1$  for Ex.1 by using method in [29].

$\eta$	$\delta x$	$\delta t$	$E_2^T$	Rate $e_2$	$E_\infty^T$	Rate $e_\infty$
1.4	$\frac{1}{4}$	0.05	$3.684945 \times 10^{-03}$	-	$4.927401 \times 10^{-03}$	-
	$\frac{1}{8}$		$9.198071 \times 10^{-04}$	2.0022	$1.257786 \times 10^{-03}$	1.9699
	$\frac{1}{16}$		$2.314130 \times 10^{-04}$	1.9908	$3.211054 \times 10^{-04}$	1.9697
1.6	$\frac{1}{4}$	0.05	$3.683697 \times 10^{-03}$	-	$4.924700 \times 10^{-03}$	-
	$\frac{1}{8}$		$9.195621 \times 10^{-04}$	2.0021	$1.257504 \times 10^{-03}$	1.9694
	$\frac{1}{16}$		$2.168473 \times 10^{-04}$	2.0842	$3.028411 \times 10^{-04}$	2.0539
1.8	$\frac{1}{4}$	0.05	$3.681100 \times 10^{-03}$	-	$4.924700 \times 10^{-03}$	-
	$\frac{1}{8}$		$9.187786 \times 10^{-04}$	2.0023	$1.256610 \times 10^{-03}$	1.9704
	$\frac{1}{16}$		$2.121292 \times 10^{-04}$	2.1147	$2.994302 \times 10^{-04}$	2.0692

Table 3: Error norms and experimental order of convergence for different values of  $\eta$  at  $T = 1$  for Ex.1 by using current technique.

$\eta$	$\delta x$	$\delta t$	$E_2^1$	Rate $e_2$	$E_\infty^1$	Rate $e_\infty$
1.4	$\frac{1}{4}$	$\frac{1}{4}$	$1.58129 \times 10^{-05}$	–	$2.24305 \times 10^{-05}$	–
1.4	$\frac{1}{8}$	$\frac{1}{8}$	$1.13824 \times 10^{-08}$	10.4401	$7.84804 \times 10^{-09}$	11.4808
1.6	$\frac{1}{4}$	$\frac{1}{4}$	$7.11714 \times 10^{-07}$	–	$5.07926 \times 10^{-07}$	–
1.6	$\frac{1}{8}$	$\frac{1}{8}$	$3.78578 \times 10^{-09}$	7.55456	$2.33549 \times 10^{-09}$	7.76475
1.8	$\frac{1}{4}$	$\frac{1}{4}$	$1.13824 \times 10^{-06}$	–	$7.84804 \times 10^{-07}$	–
1.8	$\frac{1}{8}$	$\frac{1}{8}$	$3.58285 \times 10^{-09}$	8.31148	$2.49454 \times 10^{-09}$	8.29741

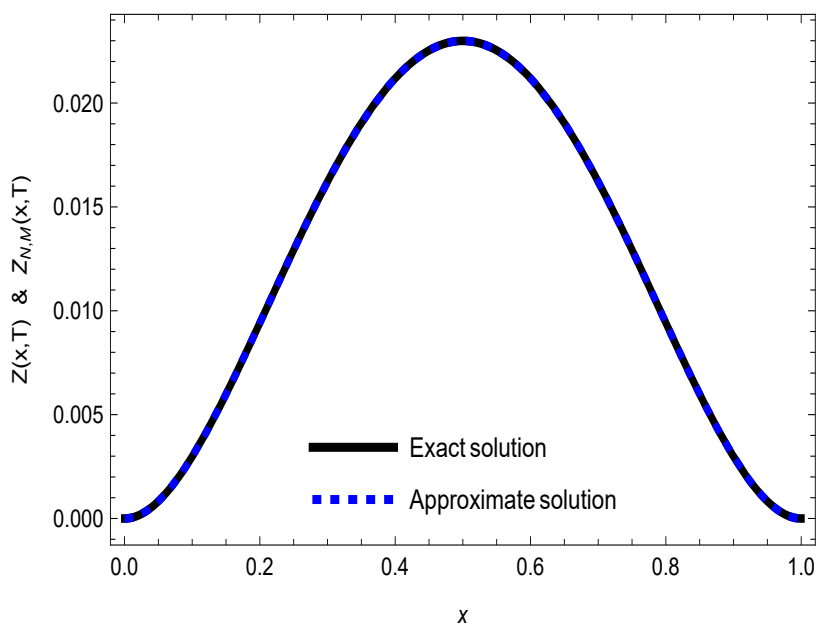


Figure 1: Comparison of between approximate solution(  $Z_{4,8}$ ) of NBOM method and exact solution for Ex.1 at  $T = 1$ .

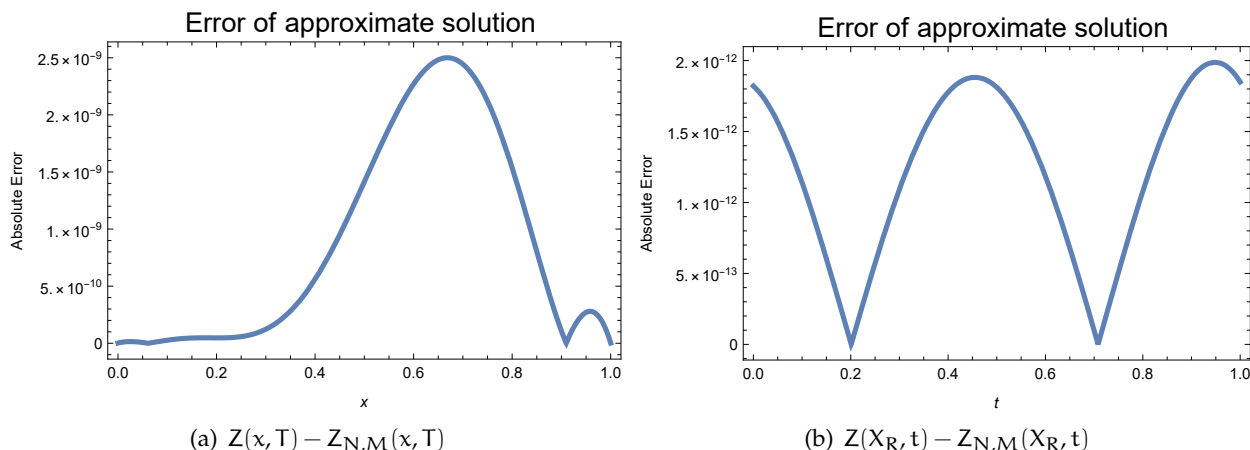


Figure 2: The absolute errors comparison between numerical solution(  $Z_{4,8}$ ) of NBOM method and exact solution for Ex.1.

Table 4: Comparison the absolute errors at some nodal points for Ex.2 with different values of  $\gamma, \zeta, \eta$  at  $T = 1$ .

$x \in [0, X_R]$ ( $Z_{2,2}$ )	Current technique $\gamma = 0.75, \zeta = 0.5, \eta = 1.8$	Current technique $\gamma = 0.9, \zeta = 0.8, \eta = 1.6$
0	$2.22 \times 10^{-16}$	$4.44 \times 10^{-16}$
0.1	$4.44 \times 10^{-16}$	0
0.2	$2.22 \times 10^{-16}$	$2.22 \times 10^{-16}$
0.3	$4.44 \times 10^{-16}$	$2.22 \times 10^{-16}$
0.4	$8.88 \times 10^{-16}$	$2.22 \times 10^{-16}$
0.5	$8.88 \times 10^{-16}$	$4.44 \times 10^{-16}$
0.6	$8.88 \times 10^{-16}$	$2.22 \times 10^{-16}$
0.7	$1.11 \times 10^{-15}$	$6.66 \times 10^{-16}$
0.8	$1.11 \times 10^{-15}$	$6.66 \times 10^{-16}$
0.9	$1.33 \times 10^{-15}$	$1.11 \times 10^{-16}$
1.0	$1.77 \times 10^{-16}$	$1.33 \times 10^{-15}$
CPU time	0.01 s	0.01 s

that the current method is much better than scheme in [28]. Figures (3) and (4) show the efficiency and the reliability of NBOM technique. By looking closely at these tables and figures, we realize that the numerical results are in the best agreement with the exact solution.

**Example 5.3.** Consider the following TSCFADE[55]:

$$\begin{aligned}
 \frac{\partial^\gamma z(x, t)}{\partial t^\gamma} &= \frac{3}{x} \frac{\partial^\eta z(x, t)}{\partial x^\eta} - \frac{1}{x} \frac{\partial^\zeta z(x, t)}{\partial x^\zeta} + h(x, t), \quad 0 < t < 1, \quad 0 < x < 2, \\
 z(x, 0) &= x^2(x - 2)^2, \quad 0 < x < 2, \\
 z(0, t) = \frac{\partial z}{\partial x}(2, t) &= 0, \quad t > 0,
 \end{aligned}
 \tag{5.3}$$

Note that  $z(x, t) = 4e^{-t}x^2(x - 2)^2$  is the exact solution.

We solve this example (Eq. (5.3)) similarly to the previous examples and obtain results, Then set up the table of maximum absolute error and CPU time needed for our method related to it (Table(5)) and also draw the Figures (5) and (6) to demonstrate its accuracy and efficiency.

**Example 5.4.** In this example, we consider the following TSCFADE[56]:

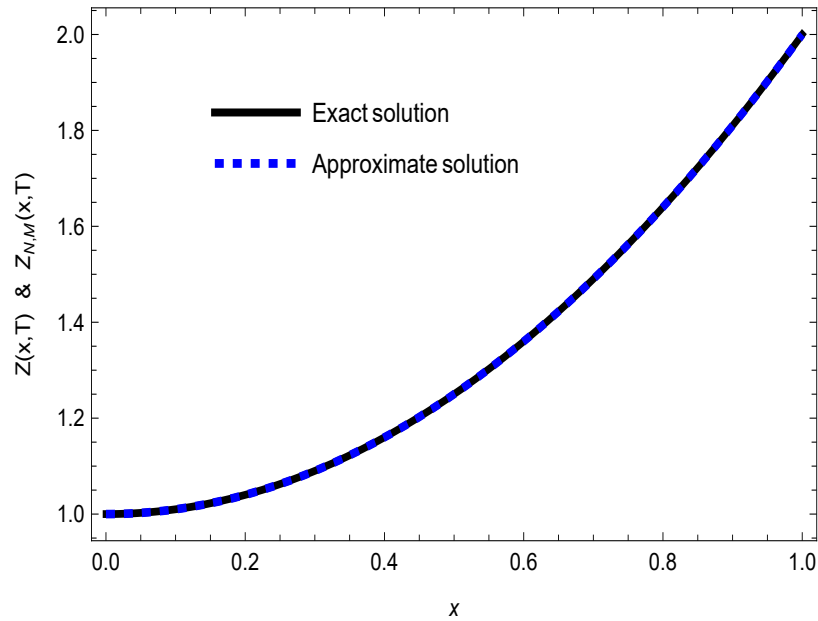


Figure 3: Comparison of between approximate solution(  $Z_{2,2}$ ) of NBOM method and exact solution for Ex.2 at  $T = 1$ .

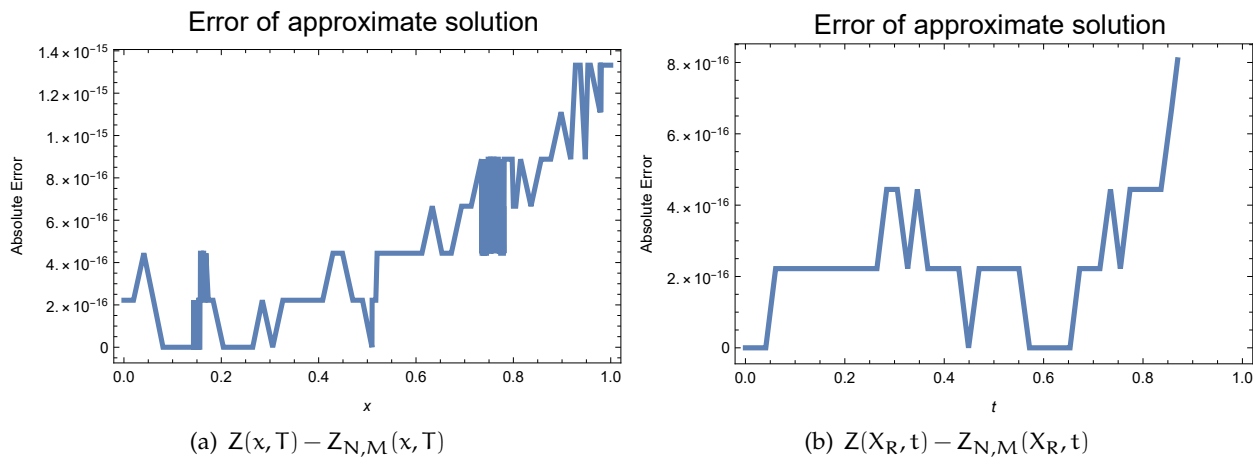


Figure 4: The absolute errors comparison between numerical solution(  $Z_{2,2}$ ) of NBOM method and exact solution for Ex.2.

Table 5: Comparison the absolute errors at some nodal points for Ex.3 with different values of  $\gamma, \zeta, \eta$  at  $T = 1$ .

$x \in [0, X_R]$ ( $Z_{4,8}$ )	Current technique $\gamma = 1, \zeta = 0.8, \eta = 1.8$	Current technique $\gamma = 1, \zeta = 0.5, \eta = 1.9$
0	$6.51 \times 10^{-13}$	$9.09 \times 10^{-13}$
0.2	$4.77 \times 10^{-8}$	$4.59 \times 10^{-8}$
0.4	$1.78 \times 10^{-7}$	$1.60 \times 10^{-7}$
0.6	$3.21 \times 10^{-7}$	$2.90 \times 10^{-7}$
0.8	$4.88 \times 10^{-7}$	$4.38 \times 10^{-7}$
1.0	$6.45 \times 10^{-7}$	$5.85 \times 10^{-7}$
1.2	$7.83 \times 10^{-7}$	$7.23 \times 10^{-7}$
1.4	$8.52 \times 10^{-7}$	$7.99 \times 10^{-7}$
1.6	$7.71 \times 10^{-11}$	$7.30 \times 10^{-7}$
1.8	$4.74 \times 10^{-10}$	$4.47 \times 10^{-7}$
2.0	$1.40 \times 10^{-10}$	$5.33 \times 10^{-12}$
CPU time	1.12 s	2.28 s

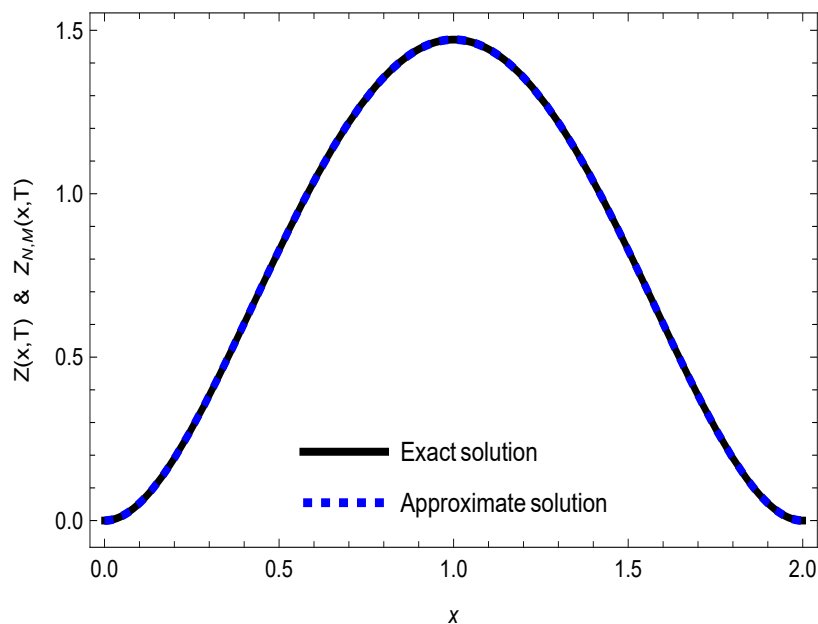


Figure 5: Comparison of between approximate solution(  $Z_{4,8}$ ) of NBOM method and exact solution for Ex.3 at  $T = 1$ .

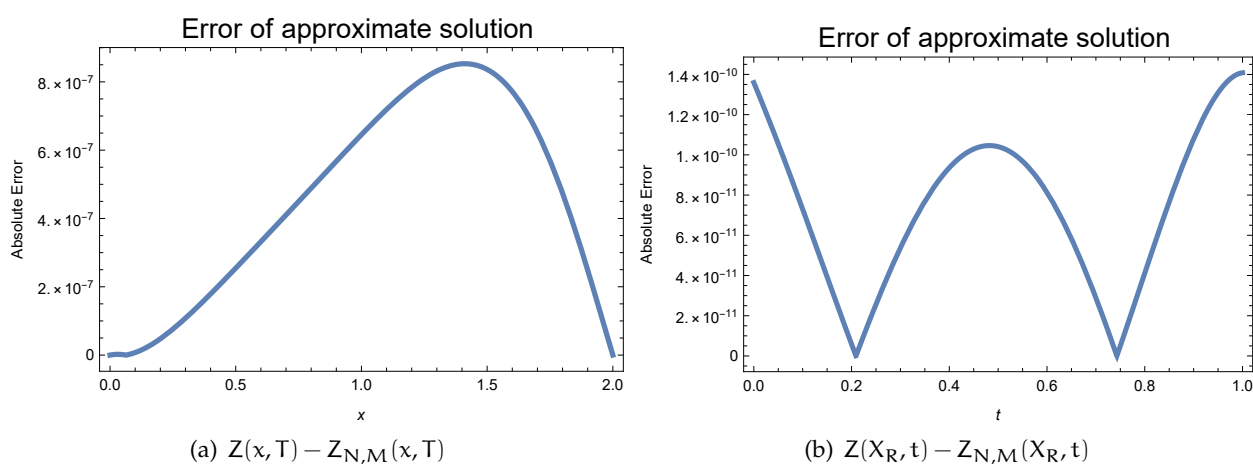


Figure 6: The absolute errors comparison between numerical solution(  $Z_{4,8}$ ) of NBOM method and exact solution for Ex.3.

Table 6: Comparison the absolute errors at some nodal points for Ex.4 with different values of  $\gamma, \zeta, \eta$  at  $T = 1$ .

$x \in [0, X_R]$ ( $Z_{3,2}$ )	Current technique $\gamma = 0.75, \zeta = 1, \eta = 2$	Current technique $\gamma = 0.6, \zeta = 1, \eta = 2$
0	$1.99 \times 10^{-15}$	$1.67 \times 10^{-15}$
0.1	$1.26 \times 10^{-14}$	$1.16 \times 10^{-14}$
0.2	$2.01 \times 10^{-14}$	$1.11 \times 10^{-14}$
0.3	$2.46 \times 10^{-14}$	$3.21 \times 10^{-15}$
0.4	$2.64 \times 10^{-14}$	$8.88 \times 10^{-15}$
0.5	$2.57 \times 10^{-14}$	$2.19 \times 10^{-14}$
0.6	$2.33 \times 10^{-14}$	$3.28 \times 10^{-14}$
0.7	$1.86 \times 10^{-14}$	$3.88 \times 10^{-14}$
0.8	$1.31 \times 10^{-14}$	$3.61 \times 10^{-14}$
0.9	$6.55 \times 10^{-14}$	$3.06 \times 10^{-14}$
1.0	$1.59 \times 10^{-15}$	$7.66 \times 10^{-15}$
CPU time	0.012 s	0.015 s

$$\begin{aligned}
 D_t^\gamma z(x, t) &= \kappa_1 D_x^\eta z(x, t) - \kappa_2 D_x^\zeta z(x, t) + h(x, t), \quad 0 < t < T, \quad 0 < x < 1, \\
 z(x, 0) &= 5x^2(1 - x), \quad 0 < x < 1, \\
 z(0, t) = z(1, t) &= 0, \quad 0 < t < T,
 \end{aligned}
 \tag{5.4}$$

Note that  $z(x, t) = 5(t^2 + 1)x^2(1 - x)$  is the exact solution,  $\kappa_1 = \kappa_2 = 1$ .

After solving this example according to the presented discussions, we obtained the result and recorded it in Table (6). We also drew Figures (7) and (8) to demonstrate its efficiency and accuracy .

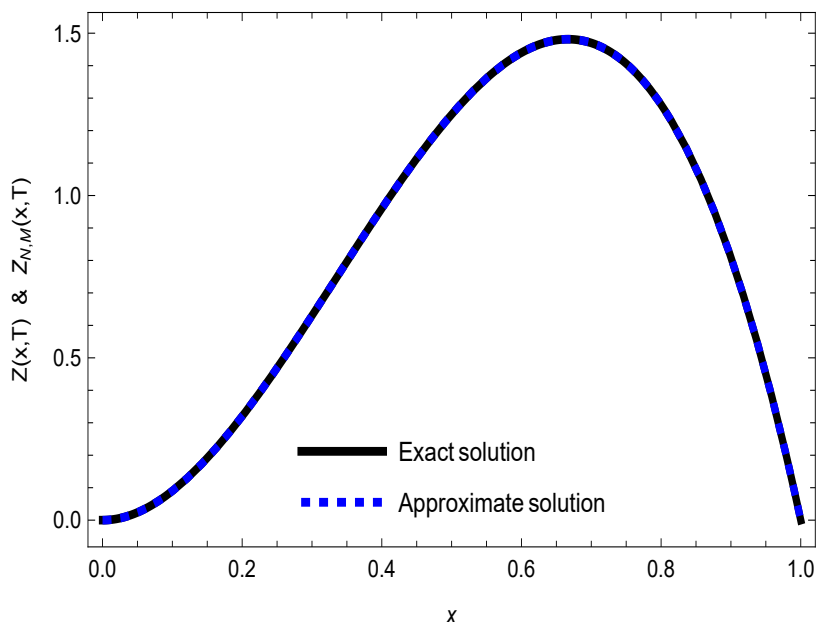


Figure 7: Comparison of between approximate solution(  $Z_{3,2}$  ) of NBOM method and exact solution for Ex.4 at  $T = 1$ .

### 6. Conclusions

In this paper, the fundamental objective of the paper is to introduce a novel computational methods based on Bernoulli operational matrix (NBOM) for time-space fractional advection-dispersion equation

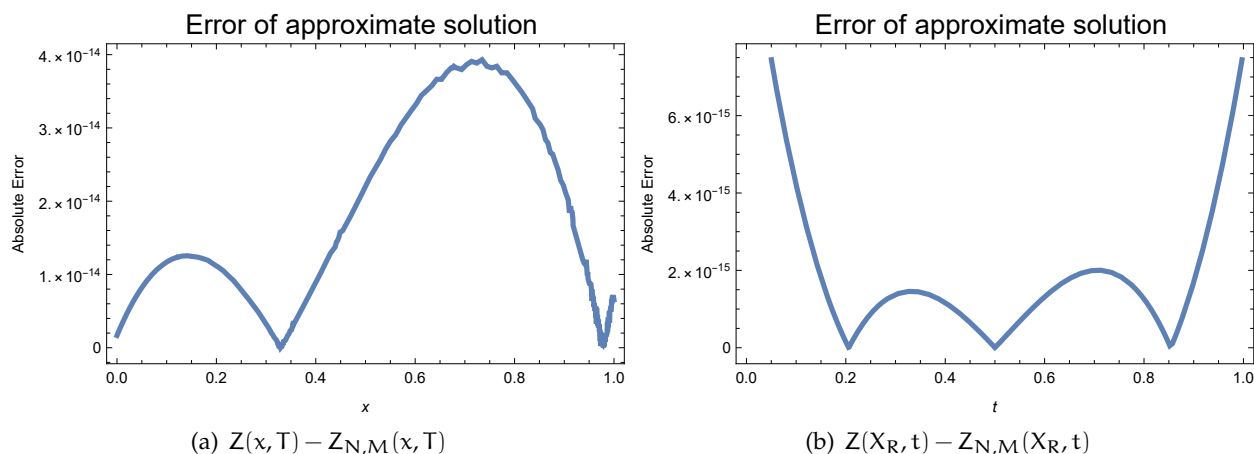


Figure 8: The absolute errors comparison between numerical solution ( $Z_{3,2}$ ) of NBOM method and exact solution for Ex.4.

(TSFAD) Eqs. (1.1)-(1.3). We investigated the generalized TSFADEs by the (NBOM) scheme. In this method, an algebraic equations system is obtained and solved by using a appropriate numerical method. The precision and effectiveness of this method is shown by solving some numerical examples. The numerical results are impressive, with low absolute errors and fast CPU times, validating the method's accuracy and practicality. The advantages of Bernoulli polynomials such as reduced computational complexity and minimized error propagation are justified.

One of the limitations of our method is that when we use a large number of nodes ( when N and M increase), the coefficient matrix becomes ill-conditioned, and a reliable solution will not be obtained.

## Acknowledgements

The authors would like to thank the anonymous reviewers for their valuable comments and helpful suggestions that improved the quality of our paper. The first author acknowledges partial support from the research grant of Imam Khomeini International University.

## References

- [1] Arfken, G., (1985). *Mathematical Methods for Physicists*, 3rd ed.; Academic Press: San Diego, CA, USA. [2.2](#), [2.2](#)
- [2] Arshad, S., Baleanu, D., Huang, J., Mohamed Al Qurashi, M., Tang, Y. & Zhao, Y., (2018). Finite Difference Method for Time-Space Fractional Advection-Diffusion Equations with Riesz Derivative, *Entropy*, 20(5) , 321. [1](#)
- [3] Agarwal, R., Yadav, M. P., Agarwal, R. P., Goyal, R. (2019). Analytic solution of fractional advection dispersion equation with decay for contaminant transport in porous media. *Matematički Vesnik*, 71(1), 5-15. [1](#)
- [4] Atabakzadeh, M.H., Akrami, M.H. & Erjaee, G.H., (2013). Chebyshev operational matrix method for solving multi-order fractional ordinary differential equations, *Appl. Math. Model.* 37 , 8903-8911. [4](#)
- [5] Baleanu, D., Magin, R.L., Bhalekar, S. & Daftardar-Gejji, V., (2015). Chaos in the fractional order nonlinear Bloch equation with delay, *Commun. Nonlinear. Sci. Numer. Simul.* 25(1-3) , 41-49. [1](#)
- [6] Bazm, S., (2015). Bernoulli polynomials for the numerical solution of some classes of linear and nonlinear integral equations, *J. Comput. Appl. Math.* 275 , 44-60. [1](#), [3](#), [4](#)
- [7] Behiry, S.H., (2014). Solution of nonlinear Fredholm integro-differential equations using a hybrid of block pulse functions and normalized Bernstein polynomials, *J. Comput. Appl. Math.* 260 , 258-265. [4](#)
- [8] Bhrawy, A.H. & Alofi, A.S., (2013). The operational matrix of fractional integration for shifted Chebyshev polynomials, *Appl. Math. Lett.* 26 , 25-31. [4](#)
- [9] Bhrawy, A.H., Tohidi, E. & Soleymani, F., (2012). A new Bernoulli matrix method for solving high-order linear and nonlinear Fredholm integro-differential equations with piecewise intervals, *Appl. Math. Comput.* 219 , 482-497. [1](#)
- [10] Bhrawy, A.H. & Zaky, M.A., (2014). A method based on the Jacobi tau approximation for solving multi-term time-space fractional partial differential equations, *J. Comput. Phys.* [1](#), [4](#)
- [11] Bojović, D. & Boško, J., (2001). Fractional order convergence rate estimates of finite difference method on nonuniform meshes, *J. Comput. Meth. Appl. Math.* 1(3) , 213-221. [1](#)
- [12] Carella, A.R. & Dorao, C.A., (2013). Least-squares spectral method for the solution of a fractional advection-dispersion equation, *J. Comput. Phys.* 232 , 33-45. [1](#)

- [13] Costabile, F., Dellaccio, F. & Gualtieri, M.I., (2006). A new approach to Bernoulli polynomials, *Rend. Mat. Ser. VII*, 26, 1-12. [2.2](#)
- [14] Dabbaghian, A. & Darzi, R., (2023). Novel existence results for sequential Caputo FDE with antiperiodic and integral boundary conditions, *Mathematics and Computational Sciences*. 4(3), 1-12. [1](#)
- [15] Danfu, H. & Xufeng, S., (2007). Numerical solution of integro-differential equations by using CAS wavelet operational matrix of integration, *Appl. Math. Comput.* 194, 460-466. [4](#)
- [16] Deng, W., (2008). Finite element method for the space and time fractional Fokker-Planck equation, *SIAM J. Numer. Anal.* 47, 204-226. [1](#)
- [17] Diethelm, K., Ford, N.J. & Freed, A. D., (2004). Detailed error analysis for a fractional Adams method, *Numer. Algorithms*. 36(1), 31-52. [1](#)
- [18] Doha, E.H., Bhrawy, A.H. & Ezz-Eldien, S.S., (2011). A Chebyshev spectral method based on operational matrix for initial and boundary value problems of fractional order, *Comput. Math. Appl.* 62, 2364–2373. [2.2](#)
- [19] Doha, E.H., Bhrawy, A.H. & Ezz-Eldien, S.S., (2012). A new Jacobi operational matrix: an application for solving fractional differential equations, *Appl. Math. Model.* 36, 4931-4943. [2.2](#)
- [20] Ervin, V.J. & Roop, J.P., (2006). Variational formulation for the stationary fractional advection-dispersion equation, *Numer. Meth. Part. Diff. Equ.* 22, 558-576. [1](#)
- [21] Galeone, L. & Garrappa, R., (2006). On multistep methods for differential equations of fractional order, *Mediterr. J. Math.* 3(3-4), 565-580. [1](#)
- [22] Gao, G.H. & Sun, H.W., (2015). Three-point combined compact difference schemes for time-fractional advection-diffusion equations with smooth solutions, *J. Comput. Phys.* 298, 520-538. [1](#)
- [23] Garrappa, R., (2015). Trapezoidal methods for fractional differential equations: theoretical and computational aspects, *Math. Comput. Simul.* 110, 96-112. [1](#)
- [24] Golbabai, A. & Sayevand, K., (2011). Analytical modelling of fractional advection-dispersion equation defined in a bounded space domain, *Math. Comput. Model.* 53, 1708-1718. [1](#)
- [25] Hejazi, H., Moroney, T. & Liu, F. (2014). Stability and convergence of a finite volume method for the space fractional advection-dispersion equation, *J. Comput. Appl. Math.* 255, 684-697. [1](#)
- [26] Hosseinzadeh, N., Shivanian, E., Fairouz, M.Z. & Chegini, T.G., (2025). A robust RBF-FD technique combined with polynomial enhancements for valuing European options in jump-diffusion frameworks, *Int. J. Dyn. Control*, 13(6), 212. [1](#)
- [27] Huang, F. & Liu, F., (2005). The fundamental solution of the space-time fractional advection-dispersion equation, *J. Appl. Math. Comput.* 19, 233-245. [1](#)
- [28] Jafari, H. & Tajadodi, H. (2015). Numerical Solutions of the Fractional Advection-Dispersion Equation, *Progr. Fract. Differ. Appl.* 1 (1), 37-45. [1](#), [5.2](#), [5.2](#)
- [29] Javadi, S., Jani, M. & Babolian, E., (2016). A numerical scheme for space-time fractional advection-dispersion equation, *Int. J. Nonlinear Anal. Appl.* 7 (2), 331-343. [1](#), [5.1](#), [5.1](#), [2](#)
- [30] Jiang, Y. & Ma, J., (2011). High-order finite element methods for time-fractional partial differential equations, *J. Comput. Appl. Math.* 235, 3285-3290. [1](#)
- [31] Keshavarz, E., Ordokhani, Y. & Razzaghi, M.A., (2016). Numerical solution for fractional optimal control problems via Bernoulli polynomials, *J. Vib. Control*. 22, 3889-3903. [1](#), [3](#), [4](#)
- [32] Khalili, Y. & Yadollahzadeh, M., (2023). On a fractional differential equation with fractional boundary conditions, *Mathematics and Computational Sciences*. 4(1), 9-17. [1](#)
- [33] Khodabandehlo, H.R., (2025). A Novel Bernoulli Operational Matrix Method for Numerical Solution of Nonlinear Multi-term Variable-order Fractional Differential Equations, *Zagros J. Appl. Math. & Data. Anal.* 1(2), 15-33. [1](#)
- [34] Khodabandehlo, H.R., Abbasbandy, S., Chegini, T.G., Shivanian, E. & Asaithambi, A., (2025). A Bernoulli operational matrix method for solving nonlinear multi-term fractional variable-order delay differential equation, *Analytical and Numerical Solutions for Nonlinear Equations*. 10(1) 1-16. [1](#)
- [35] Khodabandehlo, H.R. & Shivanian, E., (2025). Novel Computational Methods Based on Shifted Jacobi Operational Matrix for Space Fractional Diffusion Equation, *Int. J. Theor. Phys.* 64(293). [1](#)
- [36] Khodabandehlo, H. R., Shivanian, E. & Abbasbandy, S., (2022). A Novel Shifted Jacobi Operational Matrix for Solution of Nonlinear Fractional Variable-Order Differential Equation with Proportional Delays, *Int. J. Indust. Math.* 14(4), 415-432. [1](#)
- [37] Khodabandehlo, H. R., Shivanian, E. & Abbasbandy, S., (2022). A novel shifted Jacobi operational matrix method for nonlinear multi-terms delay differential equations of fractional variable-order with periodic and anti-periodic conditions, *Math. Meth. Appl. Sci.* 45(16), 10116-10135. [1](#)
- [38] Khodabandehlo, H. R., Shivanian, E. & Abbasbandy, S., (2022). Numerical solution of nonlinear delay differential equations of fractional variable order using a novel shifted Jacobi operational matrix, *Eng. with Comp. Suppl* 3(38), S2593-S2607. [1](#)
- [39] Khodabandehlo, H. R., Shivanian, E. & Abbasbandy, S., (2026). A novel shifted Jacobi operational matrix method for linear multi-terms delay differential equations of fractional variable-order with periodic and anti-periodic conditions, *Kragujevac Journal of Mathematics*. 50(1), 39-69. [1](#)
- [40] Labecca, W., Guimaraes, O. & Piqueira, J.R.C., (2014). Dirac's formalism combined with complex Fourier operational matrices to solve initial and boundary value problems, *Commun. Nonlinear Sci. Numer. Simul.* 19.8,

- 2614-2623. [4](#)
- [41] Liu, F., Zhuang, P., Anh, V., Turner, I. & Burra, K., (2007). Stability and convergence of the difference methods for the space-time fractional advection-diffusion equation, *Appl. Math. Comput.* 191 , 12-20. [1](#)
- [42] Liu, Q., Liu, F., Turner, I. & Anh, V., (2007). Approximation of the Lévy-Feller advection-dispersion process by random walk and finite difference method, *J. Comput. Phys.* 222 , 57-70. [1](#)
- [43] Lubich, C., (1984). Discretized fractional calculus, *SIAM J. Math. Anal.* 17(3) , 704-719. [1](#)
- [44] Mashayekhi, S., Ordokhani, Y. & Razzaghi, M., (2012). Hybrid functions approach for nonlinear constrained optimal control problems, *Commun. Nonlinear. Sci. Numer. Simulat.* 17 ,1831-1843. [2.2](#)
- [45] Momani, S. & Odibat, Z., (2008). Numerical Solution of the Space-Time Fractional Advection-Dispersion Equation, *Numer. Meth. Part. Differ. Equat.* 24 (6) , 1416-1429. [1](#)
- [46] Nemati, S., Lima, P. M. & Torres, D. F. M., (2019). Numerical Solution of Variable-Order Fractional Differential Equations Using Bernoulli Polynomials, *Fractal Fract.* 5 (219). [1](#), [2.2](#), [2.2](#), [3](#)
- [47] Odibat, Z., (2024). On the Numerical Discretization of the Fractional Advection-Diffusion Equation with Generalized Caputo-Type Derivatives on Non-uniform Meshes, *Commun. Appl. Math. Comput.* [1](#)
- [48] Pang, G., Chen, W. & Fu, Z., (2015). Space-fractional advection-dispersion equations by the Kansa method, *J. Comput. Phys.* 293 , 280-296. [1](#)
- [49] Ramezani, M., Mojtabaei, M. & Mirzaei, D., (2015). DMLPG solution of the fractional advection-diffusion problem, *Eng. Anal. Bound. Elem.* 59 , 36-42. [1](#)
- [50] Razzaghi, M. & Yousefi, S., (2005). Legendre wavelets method for the nonlinear Volterra-Fredholm integral equations, *Math. Comput. Simul.* 70 , 1-8. [4](#)
- [51] Saadatmandi, A., (2014). Bernstein operational matrix of fractional derivatives and its applications, *Appl. Math. Model.* 38 , 1365-1372. [4](#)
- [52] Saadatmandi, A. & Dehghan, M., (2010). A new operational matrix for solving fractional-order differential equations, *Comput. Math. Appl.* 59 ,1326-1336. [4](#)
- [53] Shirzadi, A., Ling, L. & Abbasbandy, S., (2012). Meshless simulations of the two-dimensional fractional-time convection-diffusion-reaction equations, *Eng. Anal. Bound. Elem.* 36, 1522-1527. [1](#)
- [54] Shivanian, E., Jafarabadi, A., Chegini, TG. & Dinmohammadi, A., (2025). Analysis of a time-dependent source function for the heat equation with nonlocal boundary conditions through a local meshless procedure, *Comput. Appl. Math.*, 44(6), 282. [1](#)
- [55] Shivanian, E. & Khodabandehlo, H. R., (2015). A characteristic difference method for fractional advection-dispersion flow equations, *Applied mathematics in Engineering, Management and Technology.* 3(1) , 618-630. [1](#), [5.3](#)
- [56] Soltanpour Moghadam, A., Arabameri, M. & Barfeie, M., (2022). Numerical solution of space-time variable fractional order advection-dispersion equation using radial basis functions, *Journal of Mathematical Modeling.* 10 (3) , 549-562. [1](#), [5.4](#)
- [57] Sousa, E., (2014). An explicit high order method for fractional advection diffusion equations, *J. Comput. Phys.* 278 , 257-274. [1](#)
- [58] Stokes, P.W., Philippa, B., Read, W. & White, R.D., (2015). Efficient numerical solution of the time fractional diffusion equation by mapping from its Brownian counterpart, *J. Comput. Phys.* 282 , 334-344. [1](#)
- [59] Tohidi, E., Bhrawy, A. H. & Erfani, K.A., (2013). Collocation method based on Bernoulli operational matrix for numerical solution of generalized pantograph equation, *Appl. Math. Model.* 37 , 4283-4294. [1](#)
- [60] Toutounian, F. & Tohidi, E., (2013). A new Bernoulli matrix method for solving second order linear partial differential equations with the convergence analysis, *Appl. Math. Comput.* 223 , 298-310. [1](#)
- [61] Tripathi, N.K., Das, S., Ong, S.H., Jafari, H. & Qurashi, M.A., (2016). Solution of higher order nonlinear time-fractional reaction diffusion equation, *Entropy.* 18, 329. [1](#)
- [62] Wang, K. & Wang, H., (2011). A fast characteristic finite difference method for fractional advection-diffusion equations, *Adv. Water Resour.* 34, 810-816. [1](#)
- [63] Yousefi, S.A. & Behroozifar, M., (2010). Operational matrices of Bernstein polynomials and their applications, *Inter. Systems Sci.* 32 , 709-716. [4](#)
- [64] Yuan, X., Jichun, W. & Luying, Z., (2009). Numerical solutions of time-space fractional advection-dispersion equations, *ICCES*, 9(2) , 117-126. [1](#)
- [65] Zheng, G.H. & Wei, T., (2010). Spectral regularization method for a Cauchy problem of the time fractional advection-dispersion equation, *J. Comput. Appl. Math.* 233 , 2631-2640. [1](#)